Applied Computer Science, vol. 11, no. 4, pp. 7–19

Submitted: 2015-10-29
Revised: 2015-11-27
Accepted: 2015-12-16

deep drawing, Al alloys, sheet metal, numerical simulation

Jan SLOTA[*], Ivan GAJDOS[*], Tomasz JACHOWICZ[**], Marek SISER[*], Volodymyr KRASINSKYI[***]

FEM SIMULATION OF DEEP DRAWING PROCESS OF ALUMINIUM ALLOYS

Abstract

This paper presents results of research with FEM simulation of sheet metal forming process. The two types of aluminium alloys from 5XXX and 6XXX series, which are used in automotive industry, were compared. The computer simulation and numerical analysis of deep drawing cup test were used to predict the ability of the forming of these alloys. The plasticity model Hill'90 was used for stamping simulations. The results of numerical simulation were validated by real experiment using sheet metal testing machine Erichsen 145-60. Both results were compared with regard to prediction accuracy in changes of thickness and ear profile.

1. INTRODUCTION

The increasing demands to reduce the fuel consumption of passenger cars, reduce consumption of energy and emissions released into atmosphere is a challenge for current automotive industry. Because of that the application of aluminium sheets became one of the main aspect in automotive.

[*] Technical University of Košice, Faculty of Mechanical Engineering, Institute of Technologies and Management, Mäsiarska 74 St., 04001 Košice, Slovakia, jan.slota@tuke.sk, ivan.gajdos@tuke.sk, marek.siser@tuke.sk
[**] Lublin University of Technology, Faculty of Mechanical Engineering, Department of Polymer Processing, Nadbystrzycka 36 St., 20618 Lublin, Poland, t.jachowicz@pollub.pl
[***] Lviv Polytechnic National University, Department of Chemical Technology of Plastics, S. Bandery 12 St., 79013 Lviv, Ukraine, vkrasinsky82@gmail.com

Its characteristic features, high strength, stiffness and density, excellent formability, great corrosion resistance and potential of recycling make it an ideal replacement for heavy materials, like steel and copper, in cars as a response to the requirements of weight reduction of auto body parts [1, 2].

Reduction of weight is mainly important because it is expected, that average vehicles weight will increase and automotive industry will continue to produce new models with high performances, luxury interior focused on high comfort and safety of passengers. As a rule, saved 10% of vehicle mass approximately equals a 5,5% reduction of fuel consumption.

Reduction of mass have a significant effect on fuel efficiency, for example if we are able to reduce weight of engine while maintaining the same parameters. This fact force the care manufacturers to consider using more of alternative materials (e.g. aluminium, composites or plastics) for auto body parts [1, 3].

Despite the excellent properties of aluminium, during the stamping several issues may occur. One of them is that elastic module of aluminium is about two-thirds lower that of steel and aluminium is therefore more susceptible to springback. This phenomenon is usually reduced by increasing of blank holding force, the amount of stretching and the sheet thickness. It is not always possible to increase the material thickness and increasing the blank holder force can cause disruption of material. Nevertheless it is possible to reduce the wrinkling by using the appropriate blank holding force. Also it is necessary to use appropriate lubrication for aluminium forming. The smoother texture of alumi-nium request dry, waxlike lubrication [4, 5].

This work is related to using of finite element method (FEM) for predicting of forming process of simple axis-symmetric cup. Influence of numerical model on quality of simulation results related to experimental results was compared. The thickness distribution, strain distribution, ear profile and punch forces were identified using experimental data and numerical simulation. In simulation mainly yield criteria, hardening curve and friction were considered, because these parameters have significant effect on precision of the numerical simulation results. In this work, two different aluminium alloy materials AW 6082 T6 and AW 5754 H11 were applied. It is shown, that the theoretical predictions are substantiated with experimental data from laboratory tests on a two grades of aluminium alloy sheets.

2. EXPERIMENTAL PROCEDURE

In this experiment we used two different materials from aluminium alloys, which are widely used in automotive industry mostly to obtain auto body components. Two different materials, frequently used in the car manufacturing industry were considered in this study: age hardened AW 6082 T6, which is mostly used to manufacture of outer auto body panels since it is precipitation hardened and free of Lueders bands and AW 5754 H11, which cannot be heat-treated is used for inner panel applications due to the formation of Lueders bands during forming. Thicknesses of materials were 1 mm for AW 6082 T6 and 0.8 mm for AW 5754 H11. Both materials were medium strength Al alloys with good corrosion resistance and their chemical compositions are shown in Table 1 and Table 2, respectively.

Tab. 1. Chemical composition of AW 6082 T6

Chemical composition	Mn	Fe	Mg	Si	Cu	Zn	Ti	Cr	Other
[%]	1.00	0.50	1.20	1.30	0.10	0.20	0.10	0.25	0.15

Tab. 2. Chemical composition of AW 5754 H11

Chemical composition	Mg	Mn+Cr	Mn	Si	Fe	Cr	Zn	Ti	Cu	Other
[%]	3.60	0.60	0.50	0.40	0.40	0.30	0.20	0.15	0.10	0.15

The mechanical properties of used materials were measured from tensile test. This test was carried out on universal testing machine TiraTEST 2300. The specimens used in tensile test were cut in the 0°, 45° and 90° directions related to rolling direction. Basic mechanical properties and levels of planar anisotropy are ilustrated in Table 3 and Table 4.

Tab. 3. Results from mechanical testing of AW 6082 T6

Dir.	$R_{p0,2}$ [MPa]	R_m [MPa]	A_{80} [%]	r [-]	r_m [-]	Δr [-]	n [-]	n_m [-]	Δn [-]
0°	314	342	13.7	0.528	0.588	-0.139	0.087	0.086	0.0003
45°	307	337	14.2	0.657			0.086		
90°	313	341	12.0	0.509			0.086		

Tab. 4. Results from mechanical testing of AW 5754 H11

Dir.	$R_{p0,2}$ [MPa]	R_m [MPa]	A_{80} [%]	r [-]	r_m [-]	Δr [-]	n [-]	n_m [-]	Δn [-]
0°	146	231	14.7	0.655			0.282		
45°	136	220	19.6	0.904	0.797	-0.214	0.283	0.283	- 0.0002
90°	137	221	18.8	0.723			0.283		

Deep drawing cup tests were performed on universal sheet metal testing machine Erichsen 145-60 with a tool set B2. With this test, it is possible to establish, if the material supplied corresponds to the prescribed technological properties. The equipment is shown on Figure 1. This tool set consists of cutting and drawing tools with hydraulic ejector located in the punch. The blanks were cut using the cutting tool originally equipped on machine. Diameter of the blank was 90 mm.

Fig. 1. a) universal testing machine Erichsen 145-60,
b) tool set for deep drawing cup test [source: own study]

Figure 2 shows the geometry of the tool used in deep drawing cup test. It was the symmetric tool for drawing of cylindrical cups with the die inner diameter of 52.5 mm and punch outer diameter of 50 mm. Die radius was 5 mm and punch radius was 3 mm. The drawing ratio of process was β = D/d = 1.8 mm. Applied blankholder force was constant during the whole process and set on value 8 kN. In order to minimizing of the friction coefficient and preventing of cup tearing, special lubrication by PTFE foil was applied. During the test, both of the punch and the blankholder forces were measured.

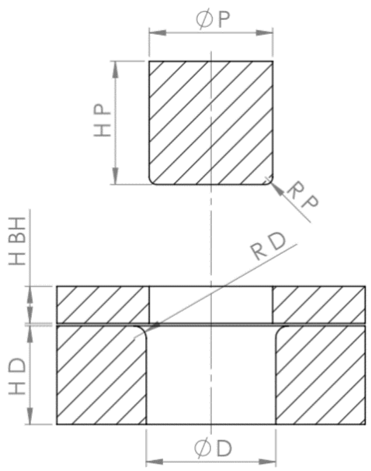

Fig. 2. Geometry of the drawing tool used in deep drawing cup test [source: own study]

It was proposed to investigate the relevance of the FEA approach to predicting the deep drawing process of an aluminium alloys, focusing on the yield criterion as numerical parameter which considerably affect the results [6].

Numerical simulation of process consists of two steps. The first step was holding the sheet metal between the die and the blankholder. The second step was drawing of cylindrical cup by the punch. FEM model of the deep drawing test with typical phases of the process is shown in Figure 3. As for the simulation of the test, the FE explicit code was used to solve the problem. Parameters of numerical simulation process are given in the Table 5.

Tab. 5. Parameters defined in explicit code of FEA

Parameter	Value	Parameter	Value
Mesh type	Triangular	Element type	Shell
Mesh size	5 mm	Friction coefficient	0,05
Level of refinement	2	Yield function	Hill90
Mesh size after refinement	1,25 mm	Hardening curve	Krupkowski
Number of integration points	5	Tool mesh	0,5 mm

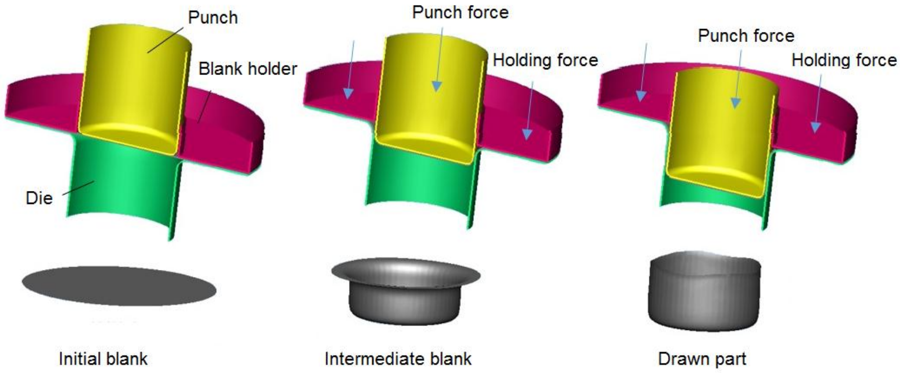

Fig. 3. Main steps of deep drawing cup test [source: own study]

The yield function define the condition for the elastic behaviour limit under multi-axial states of stress, after which the material continues deforming plastically until failure, showing a hardening behaviour. The plasticity models Hill'48 and Hill'90 are usually used for stamping simulations. The Hill'48 yield locus is based on the R-values obtained from tensile tests in three directions: 0°, 45° and 90° to the rolling direction. The Hill48 criterion cannot describe the behaviour of sheet metals with an r-value less than the unity and the yield stress under balanced biaxial tension significantly higher than the uniaxial yield stress in the plane of the sheet. This behaviour was observed for aluminium alloy sheets having an r-value under 1.0. To capture this behaviour, non-quadratic yield formulations were developed for anisotropic materials. Hill proposed a non-quadratic form called Hill'90, which requires the identification of five material parameters, four from uniaxial tensile tests and one from balanced biaxial tests [7].

Material of blank defined in numerical simulation was in the case of yield function approximated using Hill 90 yield criterion for plane stress problems with planar anisotropy, which is defined by following law:

$$\left(\frac{\sigma_1}{\sigma_0}\right)^2 + \left(\frac{\sigma_2}{\sigma_{90}}\right)^2 + \left[(p+q-c) - \frac{p\sigma_1 + p\sigma_2}{\sigma_b}\right]\left(\frac{\sigma_1\sigma_2}{\sigma_0\sigma_{90}}\right) = 1 \qquad (1)$$

where: σ_0 – uniaxial tensile yield stress in the rolling direction,

σ_{90} – uniaxial tensile yield stress in the direction normal to the rolling direction,

σ_b – yield stress under uniform biaxial tension, and *c*, *p*, *q* are parameters defined as:

$$c = \frac{\sigma_0}{\sigma_{90}} + \frac{\sigma_{90}}{\sigma_0} - \frac{\sigma_0 \sigma_{90}}{\sigma_b^2} \quad (2)$$

$$\left(\frac{1}{\sigma_0} + \frac{1}{\sigma_{90}} - \frac{1}{\sigma_b}\right) p = \frac{2R_0(\sigma_b - \sigma_{90})}{(1+R_0)\sigma_0^2} - \frac{2R_{90}\sigma_b}{(1+R_{90})\sigma_{90}^2} + \frac{c}{\sigma_0} \quad (3)$$

$$\left(\frac{1}{\sigma_0} + \frac{1}{\sigma_{90}} - \frac{1}{\sigma_b}\right) q = \frac{2R_{90}(\sigma_b - \sigma_0)}{(1+R_{90})\sigma_{90}^2} - \frac{2R_0\sigma_b}{(1+R_0)\sigma_0^2} + \frac{c}{\sigma_{90}} \quad (4)$$

where: R_0 – the R-value for uniaxial tension in the rolling direction,
R_{90} – the R-value for uniaxial tension in the in-plane direction perpendicular to the rolling direction.

According to [7], the use of Hill90 criterion is more appropriate than Hill48 for aluminium alloy and high strength steels. Advanced models like BBC2005, Corus-Vegter or Corus-Vegter Lite need a lot more test data which is not always available.

3. RESULTS AND DISCUSSION

Based on the measured mechanical properties in particular directions, we can say that the tested materials will behave very differently during forming. For achieve the best forming properties it is necessary for material to have low yield strength and also high ultimate tensile strength values, high value of elongation and ratio $R_{p0,2}/R_m$ as low as possible. The differences between max and min values in particular directions (0°, 45° and 90°) were up to 10 MPa for both materials. Coefficients of normal anisotropy r were less than the unity, what means that the strain occurs mainly as deformation in the sheet thickness.

Fig. 4. Drawn cups from materials AW 6082 T6 (left) and AW 5754 H11 (right) [source: own study]

The fully drawn cups of each material are shown in Figure 4. In the deep drawing cup test has been explored a number of parameters, as force on punch, cup height and wall thickness of drawn part. It was assumed that material AW 6082 T6 will need to deform higher force than material AW 5754 H11. The forces on punch are illustrated in Figure 5.

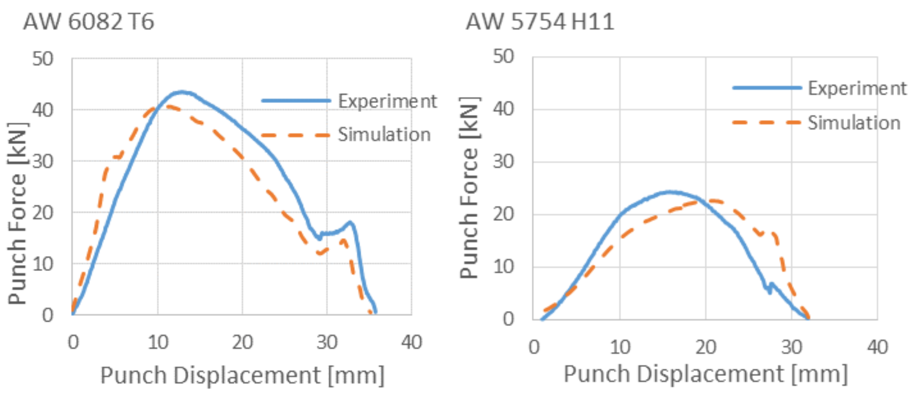

Fig. 5. Comparison of punch forces during the test [own study]

The maximum punch force for material AW 6082 T6 of 43.2 kN was obtained at the punch displacement value of 12–13 mm. In this time should be completely formed radii of a tool. The punch force decreased to value of the punch displacement at 28 mm. The force recovered due to the loss of contact between the blankholder and the die. The punch force again increase at value 32 mm because of ironing effect between the punch and the die. This was due to the increase of the blank thickness which occurred during the first forming step, when the material was strongly compressed circumferentially in the region of flange. Material AW 5754 H11 behave similarly just the maximum of the punch force was 24.3 kN and it was obtained at the punch displacement value of 15–16 mm. The force decreased to value 26 mm and then recovered to the punch displacement 28 mm.

a) b) c)

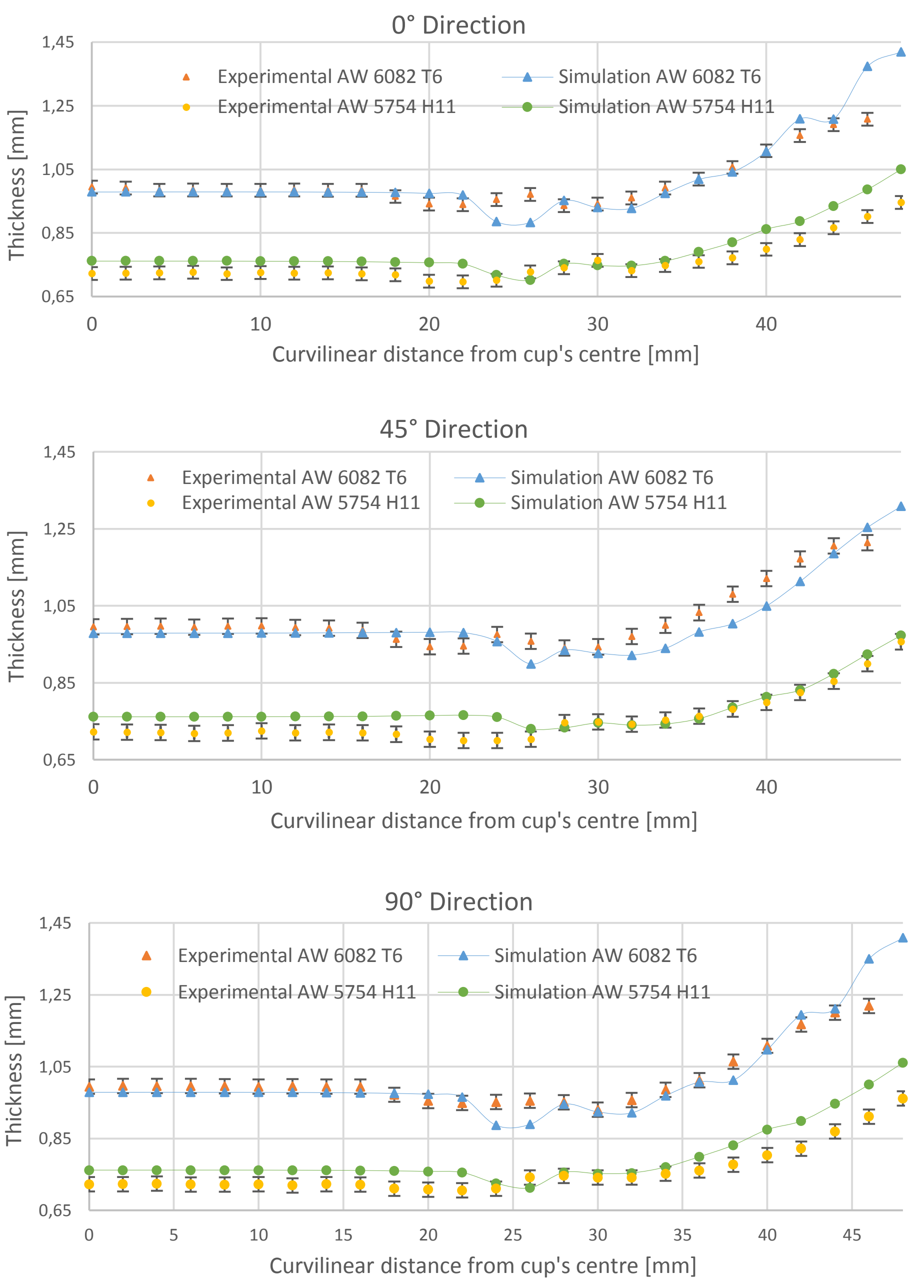

Fig. 6. Thickness distribution of the drawn cup measured at a) 0°, b) 45° and c) 90° with respect to the rolling direction [source: own study]

The thickness distribution of cup was measured too. Experimental samples were measured by micrometer in three directions and distance of measured points was 2 mm. On bottom of cups was thickness equal with value of initial blank. Closer to the radii of cup thickness starting to decrease. After the radii was completely formed thickness started to increase due to ironing effect (T6 – 141.9%, H11 – 139.9%).

The distribution of sheet thickness was compared with numerical simulation. The results are shown in Figure 6. We can see that the results from numerical simulation are very similar to values measured on real cups. The biggest differences are in the end of wall section, where thickness is influenced by ironing effect. Thickness in this areas increase rapidly, which is clearly shown in Figure 7. Results from numerical simulation are in good agreement with experimental results.

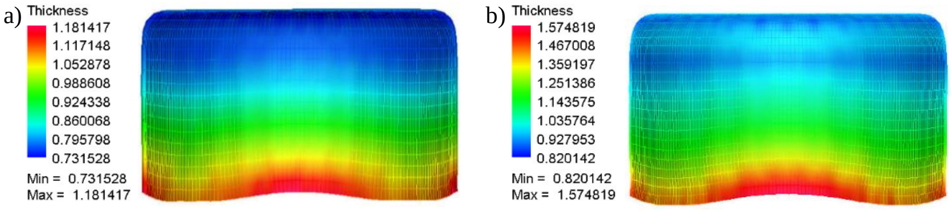

Fig. 7. Thickness distribution in drawn cups: a) AW 5754 H11, b) AW 6082 T6 [source: own study]

The cups was fully drawn without crack occurred. The area right after bend radius in the wall was the most critical due to minimal thickness of the drawn piece. Strain on the walls was high due to the ironing effect but there is no risk of fractures. Only risk on the walls was secondary wrinkling, but using appropriate blankholder force this effect was excised.

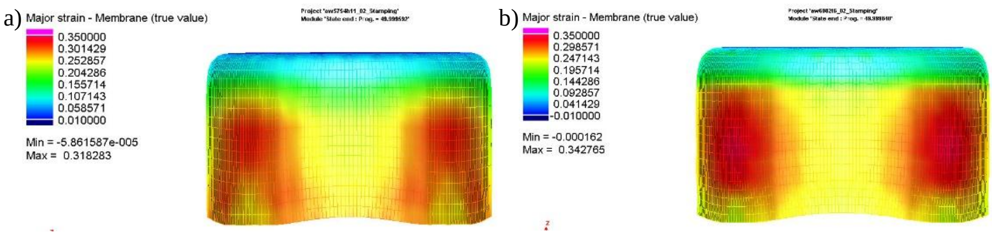

Fig. 8. Major strain distribution: a) AW 5754 H11, b) AW 6082 T6 [source: own study]

The next measured parameter was the ear profile of the cups, so the heights of cups were measured. The measurement was executed around circumference of drawn pieces with pitch of measured points after 45°. Creation of the ears is an undesirable effect of deep drawing processes and therefore materials with lower ear coefficient are more suitable for deep drawing process. The cup height is for material T6 approximately 30.11 mm whereas the punch displacement is 48 mm. For material H11 is the cup height higher with 30.26 mm and punch displacement is also 48 mm. This difference allows the cup to be fully drawn by the null value of the punch force at the end of process. The four peaks were at angles of 45°, 135°, 225° and 315° with respect to the rolling direction reached minimum height at 0° and equivalent position. No secondary peaks were observed as we can see in Figure 9.

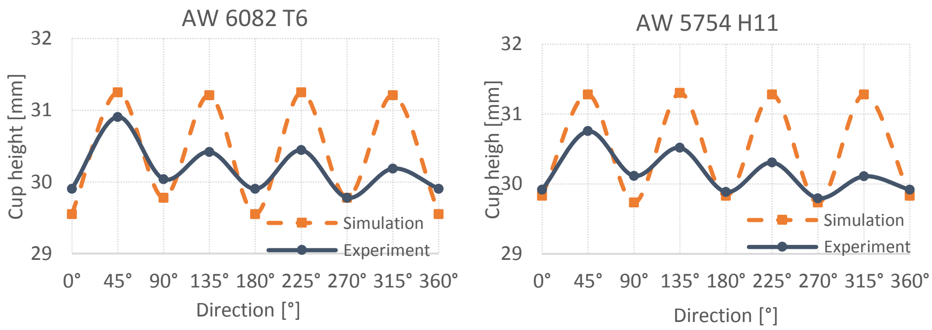

Fig. 9. Ear profile of the cups [source: own study]

The finite element analysis was used to compare results from real experiments performed on two different aluminium material with computed values from explicit solver. These results were compared in order to determine the adequacy of numerical simulation and they were the punch force, thickness distribution of cups in particular directions and ear profile of the cups.

In the case of punch force the maximum force measured during the experiment for AW 6082 T6 was 41.909 kN, while maximum force in numerical simulation was 43.193 kN (Figure 5). The overall course of forces form simulation was very similar to experiments. According to the simulation punch force increases rapidly in the beginning of the process and when the force was highest difference between simulation and experiment was around 3 kN, where simulation shown lower valued of force than was measured. The maximum force was measured at the same distance around 12–13 mm. After that the force start to decrease in the same rate in simulation and experiment and was lower around 2.5 kN in simulation.

The thickness distribution of a cups was confirmed by numerical distribution of the thickness and the ear profile is presented in Figure 9. Only the small deviations occurs in thickness distribution of the cup. The ear coefficient was computed from the equation:

$$h = \frac{h_{max} - h_{min}}{h_{min}} * 100\ [\%] \tag{5}$$

where: h_{max} – maximum ear,
h_{min} – minimum ear.

The ear coefficient of the experimental samples was 3.79% and numerical result 5.73% was little high than experiment. According to this information we can concluded, that material model set in simulation FE code is respond to behaviour of material in real conditions.

In case of the material AW 5754 H11, the punch force was 24.270 kN while maximum force in numerical simulation was 22.602 kN (Figure 5). For this material force do not fully reflect real experiment. Initially force rise in same rate as the experiment and therefore maximum force was reached later, at 15–22 mm. After reaching peak, the force gradually decreases. Position which show where the material was going out from under the blankholder appeared in the same place as during the experiment, but according to simulation the force should be much higher. The thickness distribution of a cups from AW 5754 H11 was slightly underestimate numerical distribution of the thickness and the ear profile is presented in Figure 10. The ear coefficient of experimental drawn piece was 3.22% and for the cup from numerical simulation 5.28%. This result is similar for both materials.

3. CONCLUSIONS

Influence of numerical model on simulation results was measured on simple axis-symmetric cups. Along with the numerical simulation, experiment under the same technological conditions, which served for comparison equality of results from numerical simulation and experiment was carried out. On the basis of carried out research it was shown, that model of yield criteria according to Hill48 is less proper for special alloys like Al alloys than other advanced models. Material of blank defined in numerical simulation was in the case of yield function approximated using Hill90 yield criterion. The results from numerical simulation are very similar to values measured on real cups.

The biggest differences in thickness distribution are on the end of wall section, where thickness is influenced by ironing effect. The punch force for material AW 6066 T6 was almost two-times higher compared to AW 5754 H11. The ear coefficient of experimental drawn pieces was similar for both materials and the difference between numerical simulation and real experiment about 1–2% was found.

Results from numerical simulation are in good agreement with experimental results. To reach better conformity of numerical results with experiments means keeping same technological conditions as in the real experiment and select advanced material models (especially yield criteria, friction and other), which need higher costs due to many necessary experiments, preparation of tests and data evaluation.

Acknowledgement

The authors gratefully acknowledge the financial support of the project VEGA 1/0872/14.

REFERENCES

[1] ZHOU J., WANG B., LIN J., FU L.: *Optimization of an aluminium alloy anti-collision side beam hot stamping process using a multi-objective genetic algorithm.* Archives of Civil and Mechanical Engineering, Vol. 13, 2013, pp. 401–411.

[2] ABE Y., OHMI T., MORI K., MASUDA T.: *Improvement of formability in deep drawing of ultra-high strength steel sheet by coating of die.* Journal of Mechanical Processing Technology, Vol. 214, 2014, pp. 1838–1843.

[3] MILLERW S. et al.: *Recent development in aluminium alloys for the automotive industry.* Material Science and Engineering, A280, 2000, pp. 37–49.

[4] MAO T., ALTAN T.: *Aluminium sheet forming for automotive applications. Part I.,* Stamping Journal, 2013.

[5] ZHOU J., WANG B., JIN J., FU L., MA W.: *Forming defects in aluminium alloy hot stamping of side-door impact beam.* Transactions of Nonferrous Metals Society of China, Vol. 24, 2014, pp. 3611–3620.

[6] LAURENT H., COËR J., MANACH P. Y., OLIVEIRA M. C., MENEZES L. F.: *Experimental and numerical studies on the warm deep drawing of an Al-Mg alloy.* International Journal of Mechanical Sciences, Vol. 93, 2015, pp. 59–72.

[7] BRUSCHI S. et al.: *Testing and modelling of material behaviour and formability in sheet metal forming.* CIRP Annals – Manufacturing Technology, Vol. 63, 2014, pp. 727–749.